

The Mechanism of Liquid Transport Through Swollen Polymer Membranes

D. R. PAUL and O. M. EBRA-LIMA, *Department of Chemical Engineering, The University of Texas, Austin, Texas 78712*

Synopsis

The pressure-driven transport of liquids employed in reverse osmosis has been shown to occur by a solution-diffusion mechanism in highly swollen polymer membranes. A theory based on this mechanism was successfully used earlier to correlate permeation fluxes for such membranes. Positive confirmation of this theory is provided here by direct measurement of the proposed concentration gradient. A study of the temperature dependence of the liquid diffusion coefficient in the polymer membrane has provided additional evidence of a hydrodynamic regime of diffusion in highly swollen membranes. It is also shown that the proposed ceiling flux in reverse osmosis is equal to the pervaporation flux.

INTRODUCTION

A wide range of reverse osmosis and ultrafiltration processes are emerging to effect separations ranging from desalination of sea water to concentrating and purifying proteins. All of these involve transport of a liquid through a membrane, generally polymeric, by the action of a hydrostatic pressure applied to the fluid upstream of the membrane. To be useful, the membrane must reject the solute to some extent; however, equally important, it must allow the solvent to pass. It is the latter issue which is pursued here. In some instances the solvent is transported by viscous flow through pores, but in others a mechanism of dissolution of the solvent into the membrane followed by molecular diffusion through the membrane is known to be operative. While the latter mechanism is widely recognized, very little is known about the details of how the applied upstream pressure induces this diffusion. In an earlier paper,¹ we described experiments in which pressure was used to induce diffusion of organic solvents through a highly swollen, cross-linked rubber membrane. In addition, a theory was proposed to explain these results. It considers in detail how the applied pressure induces a concentration gradient which results in a diffusion flux of the solvent. The theory is able to correlate the observed fluxes in a logical and rational fashion; however, no direct proof of the supposed concentration gradient or the conclusions that followed has been given beyond this. This paper provides this proof through direct measurement of this gradient. In addition, some tentative conclusions drawn earlier regarding the role of hydrodynamics

in the diffusion process and a possible relation between pervaporation and pressure-induced diffusion are explored further here.

EXPERIMENTAL APPARATUS

The permeation results reported previously¹ were obtained using an Amicon Model 420 cell modified to permit the permeation rate to be measured by following the rise in liquid level in a vertical capillary tube. This cell will not permit pervaporation-type experiments; hence, it was necessary to construct a new cell for this work. A schematic diagram of it is shown in Figure 1. This device can be used for both pervaporation and pressure-driven permeation measurements using a capillary to follow the progress in either instance.

The new cell consists of two stainless steel discs 6 in. in diameter, with a porous metal disc mounted in the upper one and a cavity machined into the lower one. The membrane is installed as shown in Figure 1. The direction of permeation is upward in all cases. The cavity in the lower plate acts as an upstream reservoir and contains two threaded openings, B and C, located 120° apart. This cavity will accommodate a magnetic stirring bar when needed. The porous plate collects the permeate which then flows radially to hole A with negligible resistance. The two discs are clamped together by six bolts equally spaced on a bolt circle (not shown in Fig. 1). A seal is provided by the O-ring shown.

For pressure-induced diffusion measurements using pure solvents, hole C is closed off by a valve, and a pressurized solvent reservoir is connected through hole B. Air is removed from the porous plate by applying a vacuum through hole A and then flooding with solvent, after which a graduated glass capillary is attached at this point. As permeation progresses, the solvent level in this capillary rises.

For pervaporation measurements, the graduated capillary is attached to B and a vacuum is applied through A. As permeation proceeds, the solvent level in the capillary falls. In each case the membrane was swollen to equilibrium before installation.

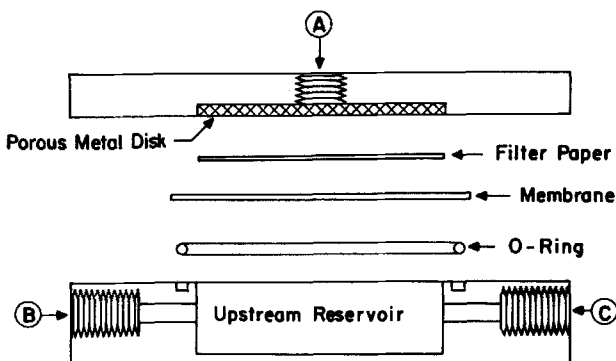


Fig. 1. Schematic diagram of apparatus used for flux measurements.

The area for permeation is defined by the porous disc and the filter paper and was 46.2 cm² here.

This design can be used with mixtures by having upstream circulation (flow through C) and stirring with a magnetic stirring bar.

DIRECT DETERMINATION OF CONCENTRATION GRADIENT

In our previous work¹ we proposed a solution-diffusion model to explain the pressure-induced diffusion of liquids through highly swollen membranes. Such a model demands a concentration gradient of the penetrant through the membrane. The theory specified that at the upstream surface, $x = 0$, the solvent volume fraction in the membrane, v_{10} , was that given by equilibrium swelling of the membrane in the solvent, while the volume fraction of solvent in the membrane at the down-stream surface, $x = l$, was *reduced* to a lower value, v_{1l} , by the action of the applied pressure. This situation follows from asserting that the pressure in the membrane, p_m , is equal to the upstream pressure p_0 . Earlier formulations of solution-diffusion models in reverse osmosis imply a different situation, namely that v_{1l} is the equilibrium swelling value and that v_{10} is *elevated* above this value by the action of the pressure. This would require p_m to be equal to the downstream pressure p_l . Both points of view result in a concentration gradient and are functionally indistinguishable from just flux measurements when $(v_{10} - v_{1l})$ is linear in $(p_0 - p_l)$, which is true at low equilibrium swelling. However, at high swelling, where the relation is highly nonlinear, there is a dramatic difference in the two. While our earlier results conformed well to our assertion, we felt that a direct measurement of the gradient would be a definitive test of our hypothesis.

We determined the concentration profile by stacking several of the membranes employed earlier into a composite membrane which was installed (preswollen) into the cell described above. Cyclohexanone was selected as the penetrant because of its low volatility and diffusion coefficient. A pressure of 400 psig was applied, and two to three days were allowed for establishment of steady-state permeation. After this time, the cell was broken apart and the membranes rapidly separated. A center section of each individual membrane was cut out and analyzed gravimetrically for its cyclohexanone content. Two separate experiments are reported here, one employing three membranes and the other, four.

The volume fraction of penetrant found in each individual membrane is of course an average value since a gradient exists in each. A quantitative comparison of these results with the theory is shown in Figure 2, where the experimental data are plotted according to the following scheme. The theoretical concentration profile in the composite membrane is given by

$$1 - v_1 = (1 - v_{10}) \left[\frac{1 - v_{1l}}{1 - v_{10}} \right]^{z/l} \quad (1)$$

where $v_{10} = 0.719$ as determined by equilibrium swelling measurements;

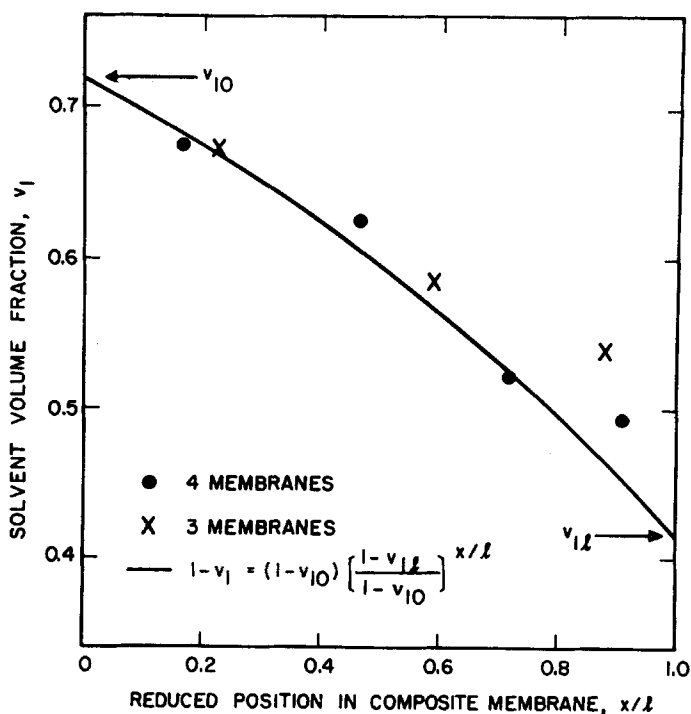


Fig. 2. Solvent concentration profile in composite membrane. Dots and crosses are experimental data, while solid line is the predicted profile. Experimental equilibrium swelling: $v_{10} = 0.719$.

$v_{1l} = 0.417$ as calculated by the thermodynamic theory proposed earlier;* and l is the thickness of the composite membrane under the conditions of the experiment, which is equal to n , the number of single membranes, times the thickness of a single membrane under the same conditions. The interfaces of the individual membranes within the composite are located at $x = 0, x_1, x_2, l$ for $n = 3$. A material balance on the membrane material reveals

$$(1 - v_{10})l_0 = \int_0^l (1 - v_1)dx = \int_0^{x_1} (1 - v_1)dx + \int_{x_1}^{x_2} (1 - v_1)dx + \int_{x_2}^l (1 - v_1)dx \quad (2)$$

where l_0 is the thickness of the composite at equilibrium swelling. Further, each of the integrals on the right must be equal to each other, since each membrane contains the same amount of polymer. Insertion of eq. (1) into eq. (2) permits the calculation of the model predicted thickness of each component membrane during diffusion. During diffusion they will not be

* Equations (12) and (13) in our earlier paper contain a misprint. The exponent on v , in the elastic term should be $1/3$, not $1/2$.

equally thick, even though originally they were. The theoretical average volume fraction of penetrant in, say, the membrane second from the top can then be calculated from

$$(\bar{v}_1)_2 = \frac{\int_{x_1}^{x_2} v_1 dx}{x_2 - x_1} \quad (3)$$

where again eq. (2) is used for v_1 in the integral. Now the experimentally determined average $(\bar{v}_1)_2$ is plotted at the position coordinate x which follows from eq. (2) when v_1 assumes the value of the average computed by eq. (3). By plotting versus x/l , the data for three- and four-membrane laminates can be placed on the same graph, thereby permitting a comparison of these data.

Figure 2 was constructed in the manner described above. The solid line is the predicted concentration profile. Note that it is not linear owing to the fact that the membrane material is stationary. The experimental data (dots and crosses) conform very well to this prediction. The largest departures are noted for the last membrane in the composite. This is to be expected, since when the pressure is released, it is the furthest from equilibrium of all the component membranes. Moreover, it is in contact with the penetrant during the disassembly of the cell and can thereby reswell. The results for the last membrane in both tests fall above the line in Figure 2, as would be expected from the above reasoning. In view of these factors, it is concluded that there is quantitative agreement between these experiments and the theory.

The above is absolute proof that the transport is by a solution-diffusion mechanism and further that the applied pressure acts to *lower* the downstream penetrant concentration rather than *raising* the upstream concentration. This is indirect evidence that the membrane pressure p_m is equal to the upstream pressure p_0 . Rosenbaum and Cotton² have considered analogous questions for the important system used in desalination, viz., cellulose acetate and water. In fact, they have reported results for the concentration profile determined in laminated membranes. Their results are less conclusive than these, because of the low swelling of water in cellulose acetate ($\sim 15\%$ at equilibrium) and the attendant experimental difficulties and inaccuracies this can cause. However, their results are in general agreement with ours.

TEMPERATURE DEPENDENCE OF PRESSURE-INDUCED DIFFUSION

By the theory described earlier,¹ diffusion coefficients were calculated from pressure-induced permeation of a variety of organic liquids through a highly swollen membrane. These diffusion coefficients correlated well with the viscosities of the solvents, suggesting a hydrodynamic regime of diffusion. If such a mechanism is operative, then the temperature dependence

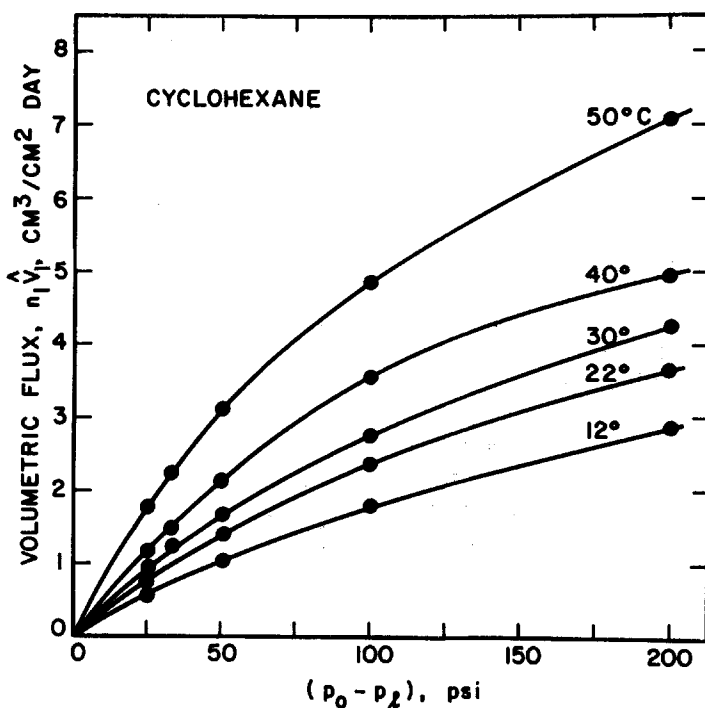


Fig. 3. Flux-pressure relationships for cyclohexane at the indicated temperatures. Experimental equilibrium swelling: $v_{10} = 0.795$.

of D for a given solvent should be related to that of the solvent viscosity. Here, we test this conclusion by examining the temperature dependence of membrane permeation using two selected solvents, viz., toluene and cyclohexane, and an identical membrane as before. Plots of the volumetric flux $n_1 \hat{V}_1$ versus the applied pressure $p_0 - p_i$ for these two solvents are shown in Figures 3 and 4. As expected, the data form a family of curves similar in shape, with higher flux levels being exhibited as the temperature is raised.

To relate the fluxes to the concentration difference generated, $v_{10} - v_{1i}$, through the theory as before, we measured the equilibrium swelling of the membrane, i.e., v_{10} , at each temperature. Only minor variations were found. Plots of $n_1 \hat{V}_1$ versus $v_{10} - v_{1i}$ were constructed as before, an example of which is shown in Figure 5. An initial linear region is seen, with a consistent departure from linearity at higher concentration differences. The direction of the departure changes with temperature and is attributed to the concentration and temperature dependence of D and χ_1 , the solvent interaction parameter. The increase in slope with temperature reflects the temperature dependence of D . The diffusion coefficients calculated from these curves¹ and similar ones for toluene are given in Figure 6.

The lower portion of Figure 6 shows these data plotted in an Arrhenius fashion, with the results being reasonably consistent with a constant activa-

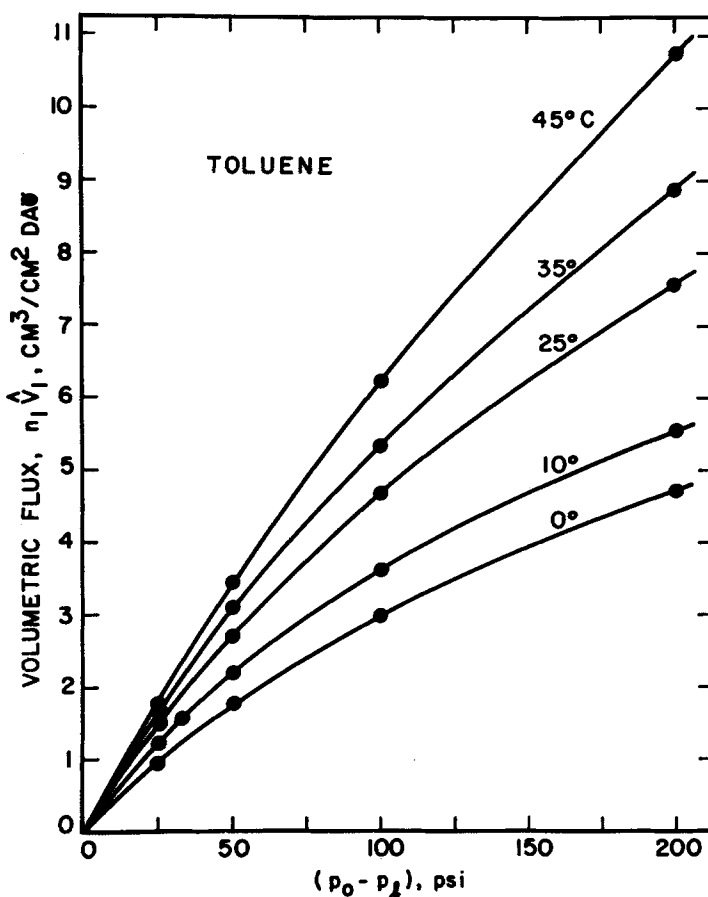


Fig. 4. Flux-pressure relationships for toluene at the indicated temperatures. Experimental equilibrium swelling: $v_{10} = 0.810$.

tion energy of 4.7 kcal/mole for cyclohexane and 2.5 kcal/mole for toluene. The two highest temperature points for cyclohexane depart from the straight-line behavior of the other points. Above 45°C with cyclohexane, bubble formation was observed on the downstream side of the cell, which is probably a result of dissolved gases and the high vapor pressure of cyclohexane at these temperatures. These bubbles could lead to erroneously high measurements of the flux, thus explaining these deviations.

Hydrodynamic theories for diffusion of particles of solutes in a solvent of viscosity η can be expressed in the simple form of $D\eta/T = a$ function of the structure of the solute (see ref. 3, for example.) The Eyring theory⁴ of self-diffusion of liquids also fits this form. The upper half of Figure 6 shows the combination $D\eta/T$ plotted versus $1/T$ where the viscosity of the solvent, cyclohexane or toluene, at the indicated temperature⁵ has been used. For toluene, $D\eta/T$ is independent of temperature within the experimental error

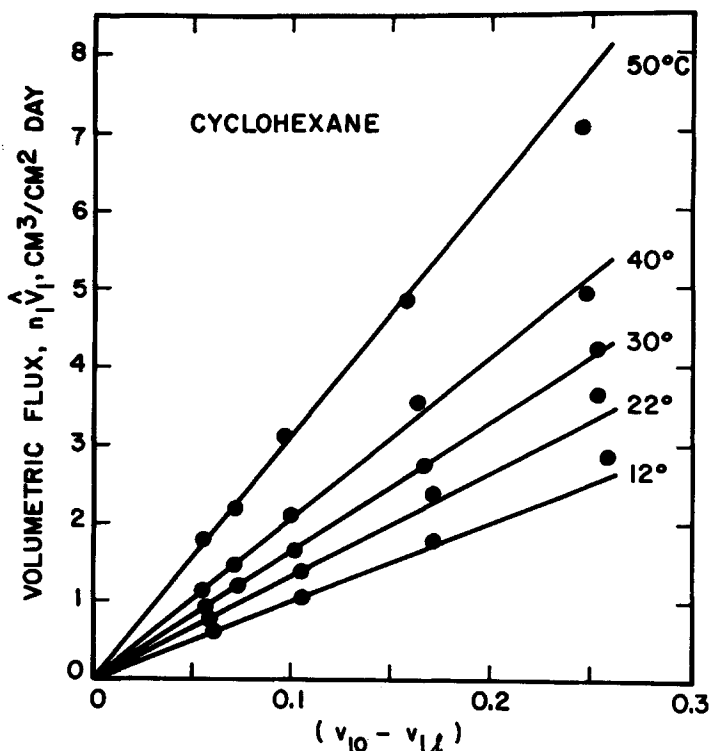


Fig. 5. Flux-concentration difference relationships for cyclohexane.

of the diffusion coefficients. For cyclohexane, there is a slight residual temperature dependence which is most exaggerated for the two points discussed above. Aside from this, the dependence is minor and hardly merits speculation at this point. It is quite important to note that the value of $D\eta/T$ is essentially the same for both solvents, in keeping with the discussion above. The temperature dependence shown here is in good accord with the suggested hydrodynamic mechanism.

We have discussed conceptually¹ how a hydrodynamic theory might be developed for a swollen polymer network analogous to the Kirkwood-Riseman theory⁶ for dilute polymer solutions. Such a theory would be consistent with the above observations. In this framework, $D\eta/T$ would be independent of the temperature and of the nature of the solvent, but would depend on the local structure and of the nature of the polymer segments. For example, bulky side groups on the chain would be expected to cause a higher hydrodynamic resistance, since they might be thought of as larger beads in the "peal string" model of the polymer chain employed in such theories.⁷ Experiments with highly swollen membranes can be visualized which would provide critical tests of this conceptual model and its utility. Even with highly swollen networks, it may be that not all factors can be explained in hydrodynamic terms.

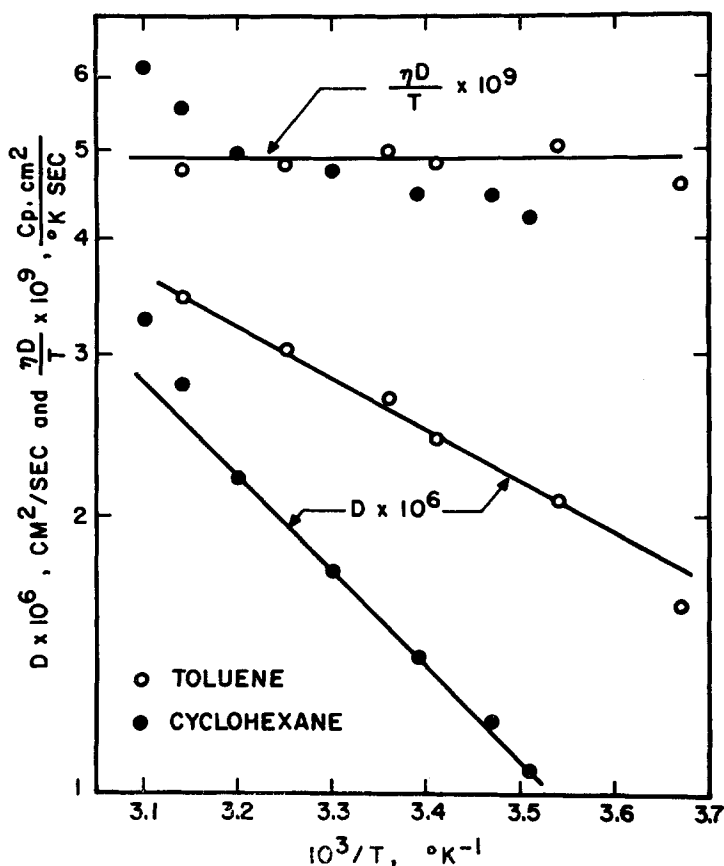


Fig. 6. Diffusion coefficient data for cyclohexane and toluene.

THE RELATION BETWEEN PERVAPORATION AND PRESSURE-INDUCED DIFFUSION

The role of the applied upstream pressure in pressure-induced diffusion is to reduce the solvent concentration at the downstream surface of the membrane, causing the concentration gradient which leads to solvent transport through the membrane. A maximum flux must result when this concentration is reduced to zero, which of course would require an infinite upstream pressure. Earlier¹ we discovered an empirical device to estimate this ceiling flux. Specifically, we noted that plots of $1/n_1 \hat{V}_1$ versus $1/(p_0 - p_i)$ formed a linear relationship for most liquids, i.e., an equation of the form

$$n_1 \hat{V}_1 = \frac{a(p_0 - p_i)}{1 + b(p_0 - p_i)} \quad (4)$$

described the data. The intercept this straight line makes upon extrapolation to $1/(p_0 - p_i) = 0$ is an estimate of the ceiling flux. In terms of eq.

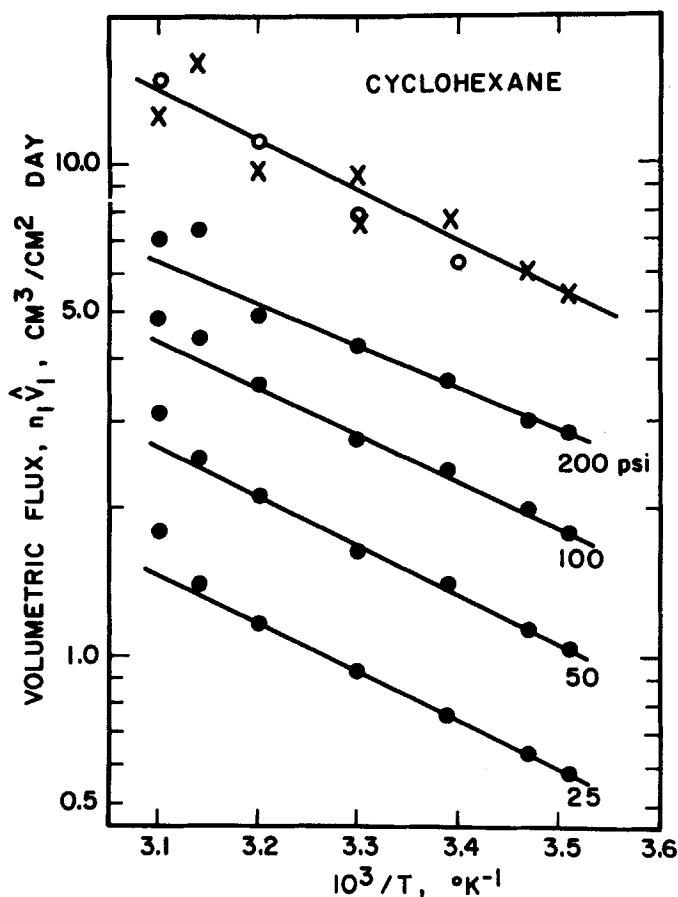


Fig. 7. Temperature dependence of cyclohexane fluxes for fixed driving forces: (●) fluxes induced by the indicated pressures; (X) ceiling flux as estimated with the aid of eq. (4); (○) pervaporation fluxes.

(4), this is a/b . The ceiling flux was determined in this way at various temperatures from the cyclohexane data reported here. The results are shown as crosses (X) in Figure 7. Similar results for the toluene data are not given since a slight curvature existed in the reciprocal plots.

As discussed previously,¹ the downstream solvent concentration v_{1l} can be made to go to zero by the mode of operation referred to by Michaels⁸ as pervaporation. It involves applying a vacuum to the downstream compartment rather than a pressure to the upstream side. The activity of the solvent in the membrane at this surface is then given by

$$a_{1l}^m = p_1/p_1^*,$$

which can be made zero by applying a sufficient vacuum so that the partial pressure of the solvent, p_1 , is very small compared to its vapor pressure, p_1^* .

As a_{1i}^m approaches zero, so does v_{1i} . In terms of this analysis, the pervaporation flux obtained under these conditions should be equal to the estimated ceiling flux from pressure-induced measurements within the ability to estimate the latter. Experimental pervaporation fluxes for cyclohexane are shown as circles (○) in Figure 7 over a range of temperatures. Comparison of the circles and crosses then demonstrates that the two are identical within the scatter of the data. The line shown corresponds to an activation energy of 4.5 kcal/mole, which is essentially the same as found for the diffusion coefficient; however, there is no general reason why this should be so. In other systems a different activation energy may result. Figure 7 also shows isobaric pressure-induced fluxes for purpose of comparison.

These results are significant in particular as they demonstrate in another way the consistency of the model for the current system. This proof is dependent on the fortuitous circumstance that the ceiling flux can be estimated via eq. (4). They are significant in general as they permit the hypothesis that the pervaporation flux is a ceiling to the pressure-induced diffusion flux for all cases, even when eq. (4) does not apply or no other suitable means for estimating this ceiling is available.

SUMMARY

The results and discussions given in the three previous sections provide ample evidence to support the proposed model for pressure-induced diffusion of liquids through highly swollen membranes. Much of the detailed thermodynamic description of the swelling behavior is applicable only to such highly swollen, nonpolar membranes when a Flory-Huggins-type relation is applicable; however, other polymer-solvent systems such as cellulose acetate-water differ only in detail and not principle. Therefore, the general features of these findings are applicable in these cases and should contribute to a better understanding of technically important processes. The observations discussed here and earlier with regard to the apparent role of hydrodynamics in determining the diffusion coefficient may not be applicable even in principle to some other systems. Highly swollen membranes have thus provided a convenient model system to pursue fundamental questions of significance to the operation of technically important membrane processes.

This work was supported in part by the National Science Foundation and the Bureau of Engineering Research at The University of Texas.

References

1. D. R. Paul and O. M. Ebra-Lima, *J. Appl. Polym. Sci.*, **14**, 2201 (1970).
2. S. Rosenbaum and O. Cotton, *J. Polym. Sci. A-1*, **7**, 101 (1969).
3. R. B. Bird, W. E. Stewart, and E. N. Lightfoot, *Transport Phenomena*, Wiley, New York, 1960, p. 513 et seq.
4. S. Glasstone, K. J. Laidler, and H. Eyring, *Theory of Rate Processes*, McGraw-Hill, New York, 1941, Chap. IX.

5. F. D. Rossini, *Selected Values of Physical and Thermodynamic Properties of Hydrocarbons and Related Compounds*, API Research Project 44, Carnegie Press, Pittsburgh, 1953.

6. J. G. Kirkwood and J. Riseman, *J. Chem. Phys.*, **16**, 565 (1948).

7. P. J. Flory, *Principles of Polymer Chemistry*, Cornell University Press, Ithaca, 1953, p. 602 et seq.

8. A. S. Michaels and H. J. Bixler, in *Progress in Separation and Purification*, Vol. I, E. S. Perry, Ed., Interscience, New York, 1968, p. 143.

Received April 12, 1971